A Proposal-Free Query-Guided Network for Grounded Multimodal Named Entity Recognition

Hongbing Li[1,†] Jiamin Liu[1,†] Shuo Zhang[1] Bo Xiao[1,*]
[1]School of Artificial Intelligence, Beijing University of Posts and Telecommunications, Beijing, China

***Abstract*—Grounded Multimodal Named Entity Recognition (GMNER) identifies named entities—including their spans and types—in natural language text and grounds them to the corresponding regions in associated images. Most existing approaches split this task into two steps: they first detect objects using a pre-trained general-purpose detector and then match named entities to the detected objects. These methods face one major limitation. The pre-trained general-purpose object detectors operate independently of textual entities, thus tend to detect common objects and frequently overlook specific, fine-grained regions demanded by named entities. This object detector-entity misalignment introduces imprecision and can impair overall system performance. In this paper, we propose a proposal-free Query-Guided Network (QGN) to unify multimodal reasoning and decoding by incorporating text guidance and cross-modal interaction. QGN enables accurate grounding and robust performance in open-domain scenarios. Extensive experiments demonstrate that QGN achieves top performance among compared GMNER models on widely used benchmarks.**

***Index Terms*—Named entity recognition, Visual grounding, End-to-end learning, Query guidance, Proposal-free grounding**

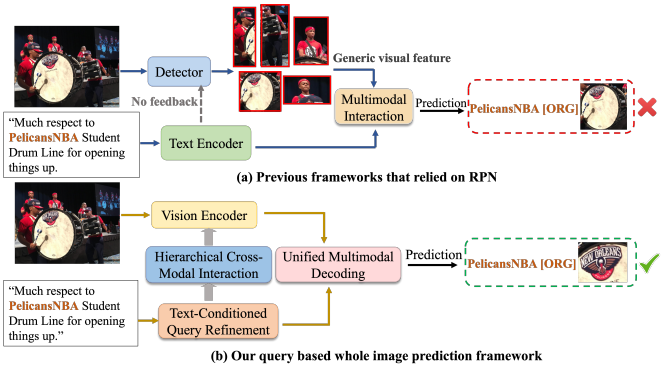

Fig. 1: Comparison of frameworks with and without candidate regions and their prediction results. (a) The detector generates many redundant areas. (b) QGN directly associates queries with the corresponding areas in the image, enabling more accurate grounding of target entities.

I. Introduction

A vast amount of multimodal information is generated every day. Social media platforms host posts that combine text, images, and videos [1]; online shopping platforms advertises using both textual descriptions and product images [2]; and hospitals routinely produce medical images accompanied by clinical narratives [3]. Efficient information search across such environments requires precise Named Entity Recognition (NER) that can operate effectively in multimodal settings.

Meeting this need demands machine learning models capable of jointly reasoning over text and images. However, conventional NER methods—designed for text alone—struggle to capture visual clues that are essential for interpreting image content [4]. To bridge this gap, Grounded Multimodal Named Entity Recognition (GMNER) has emerged as a task to jointly extract entity spans and types from text, simultaneously grounding them within images [5]. By linking textual entities to visual evidence, GMNER enables richer multimodal understanding and supports downstream applications such as multimodal retrieval [6], knowledge graph construction [7], and information extraction [8].

A central goal of GMNER is to align each identified textual entity with its corresponding visual region in the image. Most existing approaches adopt a two-step strategy: they first use a pre-trained general-purpose object detector (*e.g.*, [9], [10] to identify prominent objects, and then align each entity to one of the detected regions [5], [11], [12]. Despite their effectiveness, these methods suffer from one major limitation. Pre-trained general-purpose object detectors operate independently of textual entities. Without the guidance of textual entities, the generic detectors are limited to recognizing common, generic categories and frequently overlook specific, fine-grained regions demanded by name entities. As an example, in Fig. 1(a), although the detected regions correctly box prominent objects, they are irrelevant to target entities. Also, the detections miss crucial granular areas (*e.g.*, the team logo) required by target entities *(e.g.*, the team name "*PelicansNBA*"). This misalignment prevents the model from linking the demanded regions with named entities, leading to potential errors in downstream applications.

To address this limitation, we propose a proposal-free Query-Guided Network (aka. QGN), which introduces text guidance and an additional query embedding as dynamic semantic carriers that provide entity-specific knowledge. ***Firstly***, we introduce a text-guided query embedding refinement strategy. By aggregating textual cues into learnable query embeddings, this component provides entity-aware priors, guiding the model toward entity-relevant semantic regions rather than generic visual patterns. ***Secondly***, we design a hierarchical cross-modal interaction mechanism that injects multi-level textual cues into visual encoding, enabling text-aware visual

†These authors contributed equally to this work.
*Corresponding author.

features and strengthening fine-grained cross-modal interactions. ***Furthermore***, we construct a unified decoding space in which aligned features and queries interact iteratively. This allows the model to consolidate multimodal evidence and perform joint reasoning about fine-grained and context-dependent entities. As shown in Fig. 1(b), the model can accurately align the organization name with the fine-grained logo region. Our contributions can be summarized as follows.

- We propose QGN, a proposal-free GMNER framework. It mitigates the structural bottleneck caused by external detectors and the cross-modal semantic misalignment introduced by entity-agnostic representations.
- We introduce three mechanisms: a text-guided query refinement strategy, a hierarchical cross-modal interaction module, and a unified decoding space that helps distinguish ambiguous entities and ground fine-grained entities.
- Experiments on two Twitter benchmarks show that QGN achieves top performance among compared GMNER models. Ablation studies confirm that our modules are complementary and indispensable.

Organization. Next, Sec. II discusses related work. Then Sec. III describes our method and the proposed network architecture. Sec. IV presents empirical results on two large benchmarks. Lastly, we conclude the paper in Sec. V.

II. RELATED WORK

A. GMNER Architectural Paradigms

Existing GMNER systems mainly follow a multi-stage pipeline. They perform subtasks-NER, object detection, grounding-separately [13]–[15], which modularize the problem but causes objective misalignment, error accumulation, and limited text-to-vision interaction [16]. Other works align subtasks via re-training [5], [11], [12]. Specifically, Yu et al. [5] cast GMNER as a sequence generation task over detected regions, Wang et al. [11] improve entity-region alignment via multi-level cross-modal attention, and Tang et al. [12] incorporate inter-entity relations and multi-granularity visual cues. However, they still depend on a two-step strategy–first detecting candidate regions and then grounding entities. Jia et al. [17] use fixed entity-type queries to enable cross-modal interaction and visual grounding. However, the queries are manually defined and non-learnable. These issues highlight the need for a novel GMNER architecture where entity semantics guide visual grounding. We thus propose QGN, a proposal-free framework that supports fine-grained, cross-modal interaction.

B. Cross-Modal Interaction

The proposal-free paradigm, introduced by DETR [18] and extended by MDETR [19] and TransVG [20], employs learnable but content-agnostic queries, which is suboptimal for text-guided tasks like GMNER. Subsequent works [21] [22] improve efficiency but still lack entity-aware query semantics. Another challenge is cross-modal granularity mismatch. Late-fusion models such as CLIP [23] produce coarse global alignments, while encoder-fusion approaches like ViLBERT [24] and LXMERT [25] fuse modalities only after visual extraction, limiting text from shaping visual features early on.

To address these gaps, QGN introduces a text-guided query refinement strategy. Unlike generic fusion or content-agnostic queries, our approach actively injects textual semantics into both the visual encoding and the query initialization stages, ensuring that the model is semantically conditioned to locate target entities from the outset.

III. METHOD

Given an image $\mathbf{I}$ and a description $\mathbf{T}$, QGN predicts for each entity a quadruple $\mathbf{E}_k = \left(p_s^k,\, p_e^k,\, c^k,\, b^k\right)$. Here, entity span is denoted as $[p_s^k, p_e^k]$. The label c^k represents the entity type, and b^k is the bounding box coordinates (x, y, w, h).

A. Feature Encoding

In the Feature Encoding module, we employ ViT-B/32 [26] from the pre-trained CLIP model [23] as the vision encoder and BERT [27] as the text encoder. The vision encoder produces visual features $\mathbf{F}^v \in \mathbb{R}^{N_v \times d}$, while the text encoder outputs textual features $\mathbf{F}^t \in \mathbb{R}^{N_t \times d}$. We define learnable queries $\mathbf{Q} \in \mathbb{R}^{N_q \times d}$ that are randomly initialized. This module contains two mechanisms.

Multi-View Query Attention (MQA). Recent GMNER studies indicate that query-based reasoning is effective for modeling entity-specific semantics and inter-entity relationships [12]. However, prior methods still face challenges in distinguishing entities that have similar expression forms or appear in highly similar contextual environments. To address this issue, we introduce the MQA module, in which each query acts as a dynamic aggregator over the textual sequence, enabling different queries to focus on distinct entities and their associated contexts, as shown in Fig. 2(a).

MQA lets each query aggregate textual evidence from multiple semantic perspectives, implemented as a two-stage refinement with text-guided cross attention followed by joint self-attention. In the first stage, each query is updated in the textual semantic space so that it acquires entity-aware semantic priors. This is achieved through text-guided cross attention between the initial queries $\mathbf{Q}$ and the textual features $\mathbf{F}^t$:

$$\mathbf{Q}_{\mathrm{g}} = \mathrm{LN}\Big(\mathbf{Q} + \mathrm{Drop}\big(\mathrm{Attn}(\mathbf{Q}\mathbf{W}_q,\ \mathbf{F}^t\mathbf{W}_k,\ \mathbf{F}^t\mathbf{W}_v)\big)\Big), \quad (1)$$

the projections $\mathbf{W}_q, \mathbf{W}_k, \mathbf{W}_v$ are learnable weight matrices. We then construct a joint sequence by concatenating the textual features and the text-guided queries along the sequence dimension, $\mathbf{F}^{tq} = [\mathbf{F}^t; \mathbf{Q}_{\mathrm{g}}] \in \mathbb{R}^{(N_t+N_q)\times d}$, Multi-head self-attention is then applied to this joint representation:

$$\mathbf{C} = \mathrm{SoftMax}\left(\frac{\mathbf{Q}'(\mathbf{K}')^\top}{\sqrt{d_h}}\right)\mathbf{V}', \quad (2)$$

where $\mathbf{Q}', \mathbf{K}'$ and $\mathbf{V}'$ are linear projections of $\mathbf{F}^{tq}$, and d_h denotes the head dimension. The output $\mathbf{C}$ is split back into refined text features $\widetilde{\mathbf{F}}^t$ and refined queries $\widetilde{\mathbf{Q}}$.

Hierarchical Vision-Language Alignment (HVLA). Entities are jointly determined by text and visual evidence. To ensure

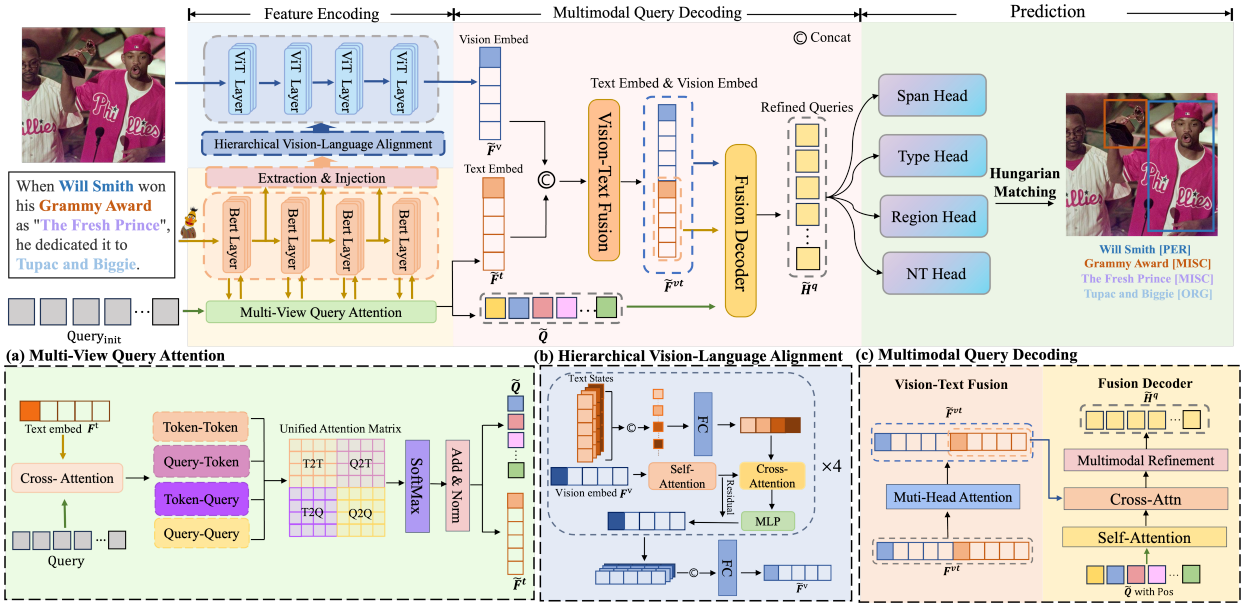

Fig. 2: **Overview of our QGN.** The input is first processed by the Feature Encoding module to obtain visual and textual embeddings along with refined queries. These are then fused in Multimodal Query Decoding and finally fed to four prediction heads. The Hungarian matching is used to select the optimal query-to-entity assignment.

that visual representations reflect entity semantics, we introduce the HVLA mechanism to align vision features with text at multiple levels, as shown in Fig. 2(b).

We extract hidden states from intermediate BERT layers indexed by $j \in J = \{1, 4, 7, 10\}$ to cover diverse semantic granularities. At each vision bridging layer indexed by $j+1$, we adaptively merge multi-layer text features. For each text layer j, the hidden state $\mathbf{F}_j^t$ is transformed by a linear projection $\widetilde{\mathbf{F}}_j^t = \mathbf{W}_j \mathbf{F}_j^t$ and combined with the original representation via a residual connection. The adapted features from all selected layers are concatenated using $\oplus$ along the feature dimension and then projected back to the original hidden size via a linear projection $\mathbf{W}_g$:

$$\mathbf{F}_{\text{fused}}^t = \mathbf{W}_g \left(\widetilde{\mathbf{F}}_1^t \oplus \widetilde{\mathbf{F}}_4^t \oplus \widetilde{\mathbf{F}}_7^t \oplus \widetilde{\mathbf{F}}_{10}^t \right). \tag{3}$$

At each bridging layer, we perform cross attention from the visual features to $\mathbf{F}_{\text{fused}}^t$ and add the result back through a residual connection. This allows visual processing to be guided by both fine-grained textual cues and global semantics at multiple stages. After encoding, we extract and concatenate visual features from ViT layers $\mathcal{V} = \{2, 5, 8, 11\}$, and map them back to dimension d, producing aligned visual embeddings $\widetilde{\mathbf{F}}^v$.

B. Multimodal Query Decoding

Although MQA and HVLA enrich text and vision features, entity cues still reside in separate spaces [28]. To alleviate this discrepancy and enable cross-modal feature reasoning, we introduce Multimodal Query Decoding (MQD), which merges enriched textual and visual queries into a shared reasoning space where queries iteratively aggregate multimodal evidence and capture inter-entity dependencies, as shown in Fig. 2(c).

Vision Text Fusion. We first concatenate visual and textual features $\mathbf{F}^{vt} = \left[\widetilde{\mathbf{F}}^v; \widetilde{\mathbf{F}}^t\right]$. The Vision Text Fusion block then applies self-attention over this joint feature with positional embeddings. This enables visual and textual elements to interact and produces an information-fused representation $\mathbf{M}^{vt}$.

Fusion Decoder. The Fusion Decoder then takes the refined queries $\widetilde{\mathbf{Q}}$ as input. Each decoder layer includes self-attention among queries and cross attention with $\mathbf{M}^{vt}$ to produce refined query representations $\mathbf{H}^q$. To strengthen the coupling of entity-centric cues before prediction, we add a Multimodal Refinement module in the Fusion Decoder. We first pool subword text features into token-level features $\mathbf{F}_{\text{tok}}^t$ using max pooling. Then we form a joint sequence $\mathbf{Z}_{\text{refine}} = [\mathbf{F}_{\text{tok}}^t; \mathbf{H}^q]$ and refine it with stacked multi-head attention layers. At the same time, the vision branch updates $\widetilde{\mathbf{F}}^v$ with synchronized layers, keeping visual features aligned with the evolving text and query context. Finally, we merge the updated visual features into the refined queries by residual fusion, producing the final query representations $\widetilde{\mathbf{H}}^q$.

C. Prediction

Multi-Head Prediction. $\widetilde{\mathbf{H}}^q$ are fed into four parallel heads. The type head produces class logits $\mathbf{z}_{\text{cls}}$ for predicting entity type c^k. Two span heads output left and right boundary scores p_{left} and p_{right}; The span (p_s^k, p_e^k) is obtained by taking the argmax of each distribution. The region head predicts normalized box coordinates $b^k = (x, y, w, h)$ to localize the visual region. The no-target head outputs logits $\mathbf{z}_{\text{nt}}$, used to identify entities. During inference, queries predicted as no-target are not matched to any visual region.

Hungarian Matching. We use the Hungarian algorithm [33] to assign each predicted query to one ground-truth entity. For an image-text pair with N_q queries and N_{gt} ground-truth entities, we build a cost matrix $C \in \mathbb{R}^{N_q \times N_{\text{gt}}}$ where entry $C_{k,j}$ combines classification, span, and region costs between

TABLE I: Performance comparison of different competitive approaches on the Twitter-GMNER datasets. Bold represents the optimal result, and underlined represents the suboptimal result.

Methods	Venue	Visual Backbone	GMNER			MNER			EEG		
			Rec.	Pre.	F1	Rec.	Pre.	F1	Rec.	Pre.	F1
GVATT-RCNN-EVG [29]	ACL'18	RN152+VinVL	47.80	48.57	49.36	78.21	74.39	76.26	54.19	52.48	53.32
UMT-RCNN-EVG [30]	ACL'20	RN152+VinVL	51.48	50.29	49.16	77.89	79.28	78.58	53.55	56.08	54.78
UMT-VinVL-EVG [30]	ACL'20	RN152+VinVL	52.52	51.31	50.15	77.89	79.28	78.58	54.35	56.91	55.60
UMGF-VinVL-EVG [31]	AAAI'21	RN152+VinVL	51.72	51.67	51.62	79.02	80.28	79.15	55.68	55.91	55.60
ITA-VinVL-EVG [32]	NAACL'22	VinVL	50.77	51.56	52.37	80.40	78.37	79.57	55.68	54.84	55.69
TIGER [11]	ACM'23	VinVL	57.45	56.63	55.84	79.88	**80.70**	80.28	60.72	61.81	61.26
H-Index [5]	ACL'23	VinVL	56.67	56.41	56.16	79.37	80.10	79.73	60.90	61.46	61.18
MNER-QG [17]	AAAI'23	DN53 + FPN	54.84	53.91	53.02	78.16	78.59	79.57	58.48	56.59	57.52
MQSPN [12]	AAAI'25	ViT-B/32+VinVL	58.49	58.76	59.03	**81.22**	79.66	80.43	61.86	62.94	62.40
QGN (Ours)	-	ViT-B/32	**59.35**	**63.23**	**61.18**	81.21	79.84	**80.52**	**65.75**	**69.25**	**67.45**

TABLE II: Comparison of F1 scores on different fine-grained types compared to previous end-to-end methods on the FMNERG dataset.

Entity Type	H-Index	TIGER	MQSPN	QGN
Person	45.13	43.78	48.64	**68.25**
Location	62.33	67.69	71.03	**72.83**
Building	32.88	40.00	**44.78**	40.62
Organization	46.68	46.75	49.03	**55.15**
Product	28.19	27.38	29.46	**32.91**
Art	38.89	43.27	42.84	**43.56**
Event	45.56	48.39	**51.88**	45.19
Other	41.81	**48.28**	43.49	34.65
All	46.55	47.20	48.57	**49.15**

query k and entity j. The classification cost is the negative logit probability for the true class y_j. The span cost is the negative sum of start and end probabilities at the ground-truth boundaries (ℓ_j, r_j) from the query's boundary distributions. The region cost uses ℓ_1 distance and IoU loss between the predicted box and ground-truth box t_j. For entities without visual regions, we mask region costs with a large constant so matching relies only on classification and span. Unmatched queries are treated as background and supervised as no-target during training. The final cost matrix is defined as:

$$C_{k,j} = \lambda_{\text{cls}} c_{\text{cls}}(k,j) + \lambda_{\text{span}} c_{\text{span}}(k,j) + \lambda_{\text{IoU}} c_{\text{IoU}}(k,j) + \lambda_{\ell_1} c_{\ell_1}(k,j). \tag{4}$$

D. Training Objective

Prediction Loss. The model is trained with a unified objective on query-entity pairs assigned via Hungarian matching. We jointly supervise each matched query's predictions of entity type, text span, and visual region using cross-entropy for classification, binary cross-entropy on left and right span boundaries, and L_1 plus generalized IoU loss for box regression. We denote the total as prediction loss $\mathcal{L}_{\text{pred}}$.

No-target Loss. The no-target loss $\mathcal{L}_{\text{nt}}$ trains a binary classifier to identify queries referring to entities without visual regions. For each matched query i, we set label $y_i^{\text{nt}} \in \{0, 1\}$ based on whether a ground-truth box exists, and apply cross-entropy over its no-target logits.

Consistency Loss. The consistency loss $\mathcal{L}_{\text{con}}$ enforces agreement among queries sharing the same text span on their no-target decisions. We group queries by span and ground-truth region index, assign a unified label per group such that the group is labeled as has-target if any member has a valid region and as no-target otherwise, and apply cross-entropy on their no-target logits.

TABLE III: The ablation studies of the proposed components.

MQA	HVLA	MQD	△	GMNER
✓	✗	✗	-2.76	58.42
✗	✓	✗	-1.61	59.57
✗	✗	✓	-1.39	59.79
✓	✓	✗	-2.16	59.02
✓	✗	✓	-0.64	59.54
✗	✓	✓	-1.92	59.26
✓	✓	✓	-	**61.18**

Overall objective. The total loss is computed as a weighted sum of the individual loss components:

$$\mathcal{L}_{\text{total}} = \lambda_{\text{pred}} \mathcal{L}_{\text{pred}} + \lambda_{\text{nt}} \mathcal{L}_{\text{nt}} + \lambda_{\text{con}} \mathcal{L}_{\text{con}}. \tag{5}$$

IV. EXPERIMENTS

A. Implementation Details

We conduct experiments on the Twitter-GMNER [5] and Twitter-FMNERG [11] datasets. All experiments are run on 2 NVIDIA RTX3090 GPUs with PyTorch 2.4.1. We use a pre-trained BERT-based model as the text encoder and ViT-B/32 from the pre-trained CLIP model as the visual encoder. For training, we set the batch size to 16, the learning rate to 2×10^{-5}, and train for 50 epochs. We use the Adam optimizer with a linear warmup ratio of 0.05.

B. Main Results

Besides the main GMNER task, we additionally report two subtasks of GMNER: Multimodal NER (MNER), which predicts entity spans and types, and Entity Extraction & Grounding (EEG), which extracts entity span and entity region pairs. Table I compares our method with representative baselines on Twitter-GMNER. QGN outperforms the proposal-free baseline MNER-QG on all tasks, owing to its entity-aware learnable queries. Moreover, QGN outperforms the

TABLE IV: The ablation results of losses evaluated by F1.

$\mathcal{L}_{\text{pred}}$	$\mathcal{L}_{\text{nt}}$	$\mathcal{L}_{\text{con}}$	△	GMNER
✓	✗	✗	-12.11	49.07
✓	✓	✗	-1.17	60.01
✓	✗	✓	-11.53	49.65
✓	✓	✓	-	**61.18**

TABLE V: The ablation results on MQA and MQD evaluated by F1.

Module	Settings	△	GMNER
MQA	Batch-Shared Query Parameters	-1.37	59.81
	Mean-Pooled Text Queries	-1.88	59.30
	Attention-Pooled Text Queries	-3.88	57.30
	w/o TQC	-1.17	60.01
	w/o JCA	-1.19	59.99
MQD	w/o VTF	-3.83	57.35
	w/o FDE	-0.98	60.20
	w/o MRE	-5.5	55.68

previous state-of-the-art model MQSPN by +2.15%, +0.09%, and +5.05% F1 score on GMNER, MNER, and EEG, respectively. These improvements indicate that removing predefined region proposals helps the model learn more accurate text-image alignments and generalize better in open-domain settings. The small gap between our GMNER and MNER scores further suggests that QGN achieves relatively accurate visual grounding and improves multimodal entity localization.

C. Performance on Fine-Grained GMNER

The Twitter-FMNERG dataset provides a more fine-grained categorization of entity types based on the GMNER dataset. We evaluate different models on the Twitter-FMNERG. The results in Table II show that QGN achieves the best performance on most entity types. It attains improvements of +19.61%, +1.80%, +6.12%, +3.45%, +0.29%, and +0.58% F1 score on *Person, Location, Organization, Product, Art*, and *All* categories, respectively. These results suggest that QGN effectively captures cross-modal semantic distinctions and supports fine-grained entity classification.

D. Ablation Studies

Effect of Module Combinations. To assess the contribution of each component, we conduct a full ablation study over all combinations of the three main modules, as shown in Table III. When used individually, MQA leads to a 2.76% drop, suggesting that refined queries alone are insufficient for capturing complete multimodal cues. Using only HVLA or only MQD results in 1.61% and 1.39% declines, showing that removing cross-modal alignment or multimodal interaction weakens the model's ability to link text with their visual evidence. For pairwise combinations, MQA+HVLA and MQA+MQD incur 2.16% and 0.64% declines, while HVLA+MQD yields a 1.92% drop. These results suggest that the three modules are mutually complementary, since any single module or pair recovers only part of the performance, whereas combining all three yields the best results.

Effect of the Loss Components. As shown in Table IV, the prediction loss $\mathcal{L}_{\text{pred}}$ provides the essential supervision and forms the foundation of our training objective. Removing the consistency loss $\mathcal{L}_{\text{con}}$ causes a moderate drop, indicating that enforcing agreement among span-sharing queries benefits region prediction. Removing the no-target loss $\mathcal{L}_{\text{nt}}$ leads to a much larger decline, showing that this supervision is crucial for distinguishing text-only entities from visually grounded ones and maintaining stable multimodal learning.

TABLE VI: The ablation results on HVLA evaluated by F1.

Extraction Stride	Extraction Start layer	Injection Stride	Injection Start layer	GMNER
3	1	3	2	**61.18**
1	1	3	2	58.87
2	1	3	2	59.88
3	2	3	2	59.78
3	3	3	2	59.36
3	1	1	2	58.76
3	1	2	2	59.11
3	1	3	1	59.59
3	1	3	3	59.32

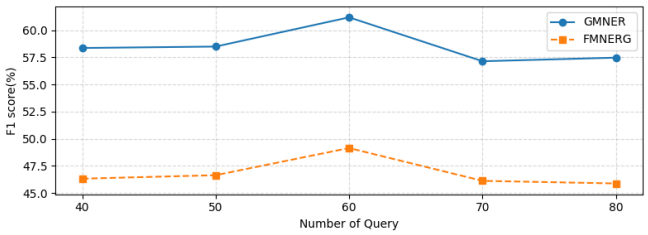

Fig. 3: Analysis of queries quantity.

Effect of the MQA Design. We evaluate the contributions of different components within MQA, as shown in Table V. Alternative query initialization strategies consistently underperform random initialization, indicating that fixed or pooled initial states restrict entity-specific modeling. Removing the text-query cross attention (w/o TQC) or the joint concatenation with its self-attention refinement (w/o JCA) further reduces performance by 1.17% and 1.19%, respectively, suggesting that both text-guided query refinement and joint token-query attention are essential for learning discriminative and context-aware query representations.

Effect of the HVLA Configuration. To analyze how hierarchical selection influences alignment quality, we vary the start layer and stride for extraction and injection. In Table VI, the first row gives the best configuration. For each subsequent pair of rows, only one variable is changed while the other three remain fixed. The changed variable appears in gray along the diagonal. The results show that starting extraction earlier and using a broader stride enables information to be collected and injected across a wider semantic range and achieves the best performance. Therefore, our final model adopts extraction layers [1,4,7,10] and injection positions [2,5,8,11].

Effect of the MQD Design. Finally, we ablate the components of MQD, as shown in Table V. Removing the Vision Text Fusion (w/o VTF) leads to a 3.83% decrease, indicating that early joint fusion of visual and textual features is important for building strong multimodal representations. Removing the Fusion Decoder (w/o FDE) causes a drop of 0.98%, showing that the dedicated query decoder provides complementary

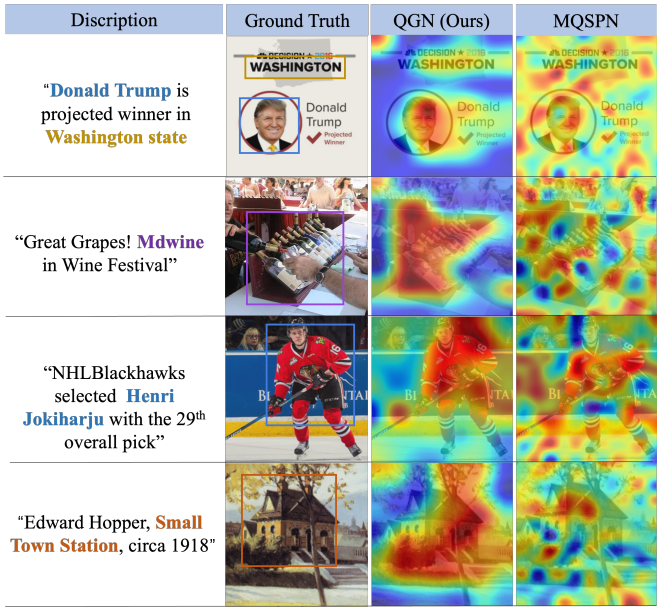

Fig. 4: Comparison of visual attention maps produced by QGN and MQSPN on the Twitter-GMNER dataset.

modeling capacity. The largest performance drop occurs when the Multimodal Refinement module is removed (w/o MRE), highlighting that iteratively refining queries with token-level text and updated visual cues is crucial for accurate prediction.

Analysis of query quantity. To explore how query quantity influences model performance, we evaluate different settings on both datasets. As shown in Fig. 3, we find that too few queries reduce F1 due to limited semantic coverage. F1 peaks at 60 queries, then declines as redundancy increases, indicating that a moderate query count is optimal.

E. Visualization Results

We visually compare the attention maps of QGN and MQSPN under various examples in Fig. 4. MQSPN often tends to highlight entity-irrelevant regions, resulting in diffuse and noisy attention patterns, whereas QGN produces sharper, localized activations around entity-relevant areas, leading to more precise predictions.

V. CONCLUSION

In this paper, we introduce QGN, a query-conditioned GMNER framework that addresses the cross-modal misalignment in existing approaches. Through text-guided query refinement, hierarchical vision-language alignment, and unified multimodal decoding, our method enables stronger multimodal reasoning and more precise entity grounding. Experiments on multiple benchmarks show that QGN achieves top performance and captures fine-grained multimodal cues, highlighting the advantages of query-guided reasoning.

REFERENCES

[1] Wentao Han et al., "A comparative analysis on weibo and twitter," *Tsinghua Science and Technology*, vol. 21, no. 1, pp. 1–16, 2016.

[2] Wei Di et al., "Is a picture really worth a thousand words? -on the role of images in e-commerce," in *ACM*, 2014, pp. 633–642.

[3] Maleki Varnosfaderani et al., "The role of ai in hospitals and clinics: transforming healthcare in the 21st century," *Bioengineering*, vol. 11, no. 4, pp. 337, 2024.

[4] Feng Chen et al., "Learning implicit entity-object relations by bidirectional generative alignment for multimodal ner," in *ACM MM*, 2023.

[5] Jianfei Yu, Ziyan Li, Jieming Wang, and Rui Xia, "Grounded multimodal named entity recognition on social media," in *ACL*, 2023.

[6] Xinyu Wang et al., "Named entity and relation extraction with multimodal retrieval," in *EMNLP*, 2022.

[7] Shenyi Qian et al., "A survey on multimodal named entity recognition," in *ICIC*, 2023.

[8] Ye Liu et al., "Mmkg: multi-modal knowledge graphs," in *ESWC 2019*, 2019.

[9] Pengchuan Zhang et al., "Vinvl: Revisiting visual representations in vision-language models," in *CVPR*, 2021.

[10] Shaoqing Ren et al., "Faster r-cnn: Towards real-time object detection with region proposal networks," *TPAMI*, 2016.

[11] Jieming Wang et al., "Fine-grained multimodal named entity recognition and grounding with a generative framework," in *ACM*, 2023.

[12] Jielong Tang et al., "Multi-grained query-guided set prediction network for grounded multimodal named entity recognition," in *AAAI*, 2025.

[13] Jinyuan Li et al., "Llms as bridges: Reformulating grounded multimodal named entity recognition," in *ACL (Findings)*, 2024.

[14] Jinyuan Li et al., "Advancing grounded multimodal named entity recognition via llm-based reformulation and box-based segmentation," *CoRR*, 2024.

[15] Hua Zhang et al., "Bridging demonstration and multi-source attention fusion using llms for grounded multimodal named entity recognition," *Information Fusion*, p. 103800, 2025.

[16] Yen-Chun Chen et al., "Uniter: Universal image-text representation learning," in *ECCV*, 2020.

[17] Meihuizi Jia et al., "Mner-qg: An end-to-end mrc framework for multimodal named entity recognition with query grounding," in *AAAI*, 2023.

[18] Nicolas Carion et al., "End-to-end object detection with transformers," in *ECCV*, 2020.

[19] Aishwarya Kamath et al., "Mdetr-modulated detection for end-to-end multi-modal understanding," in *ICCV*, 2021.

[20] Jiajun Deng et al., "Transvg: End-to-end visual grounding with transformers," in *ICCV*, 2021.

[21] Xizhou Zhu et al., "Deformable detr: Deformable transformers for end-to-end object detection," in *ICLR*, 2021.

[22] Hao Zhang et al., "Dino: Detr with improved denoising anchor boxes for end-to-end object detection," in *The Eleventh International Conference on Learning Representations*, 2023.

[23] Alec Radford et al., "Learning transferable visual models from natural language supervision," in *ICML*, 2021.

[24] Jiasen Lu, Dhruv Batra, and Devi Parikh, "Vilbert: Pretraining task-agnostic visiolinguistic representations for vision-and-language tasks," *Advances in neural information processing systems*, vol. 32, 2019.

[25] Hao Tan and Mohit Bansal, "Lxmert: Learning cross-modality encoder representations from transformers," in *EMNLP-IJCNLP*, 2019.

[26] Alexey Dosovitskiy et al., "An image is worth 16x16 words: Transformers for image recognition at scale," in *International Conference on Learning Representations*, 2021.

[27] Jacob Devlin, Ming-Wei Chang, Kenton Lee, and Kristina Toutanova, "Bert: Pre-training of deep bidirectional transformers for language understanding," in *NAACL*, 2019.

[28] Yuxiao Chen et al., "Revisiting multimodal representation in contrastive learning: from patch and token embeddings to finite discrete tokens," in *CVPR*, 2023.

[29] Di Lu et al., "Visual attention model for name tagging in multimodal social media," in *ACL*, 2018.

[30] Jianfei Yu, Jing Jiang, Li Yang, and Rui Xia, "Improving multimodal named entity recognition via entity span detection with unified multimodal transformer," in *ACL*, 2020.

[31] Dong Zhang et al., "Multi-modal graph fusion for named entity recognition with targeted visual guidance," in *AAAI*, 2021.

[32] Xinyu Wang et al., "Ita: Image-text alignments for multi-modal named entity recognition," in *NAACL*, 2022.

[33] Harold W Kuhn, "The hungarian method for the assignment problem," *Naval Research Logistics (NRL)*, vol. 52, no. 1, pp. 7–21, 2004.